THE JOURNAL OF BIOLOGICAL CHEMISTRY
Vol. 279, No. 26, Issue of June 25, pp. 27699–27708, 2004
Printed in U.S.A.

The Murine *Irak2* Gene Encodes Four Alternatively Spliced Isoforms, Two of Which Are Inhibitory*

Received for publication, March 19, 2004
Published, JBC Papers in Press, April 13, 2004, DOI 10.1074/jbc.M403068200

Matthew P. Hardy and Luke A. J. O'Neill‡

From the Department of Biochemistry and the Biotechnology Institute, Trinity College Dublin, Dublin 2, Ireland

The interleukin-1 receptor-associated kinases (IRAKs) are important downstream signaling components of Toll-like receptors (TLRs). To date, four mammalian IRAKs have been found, namely IRAK-1, IRAK-2, IRAK-4, and IRAK-M. Herein, we show a detailed analysis of the genomic region encompassing the murine *Irak2* gene and the molecular cloning of four isoforms of Irak2 (designated Irak2a, Irak2b, Irak2c, and Irak2d) generated by alternative splicing at the 5′-end of the gene. This alternative splicing has direct effects on the expression of the N-terminal death domain and/or interdomain. No evidence of similar alternative splicing was found for the human *IRAK2* gene. When overexpressed, Irak2a and Irak2b potentiated NF-κB activation by lipopolysaccharide. Importantly, Irak2c and Irak2d were inhibitory. The promoter for Irak2c differed from that of the other Irak2 isoforms in that it contained putative NF-κB binding sites. Lipopolysaccharide induced the expression of Irak2c, indicating a possible negative feedback effect on the signaling pathway. Alternative splicing of the *Irak2* gene in mice will therefore generate agonistic or antagonistic Irak2 isoforms, which is likely to have consequences for the regulation of TLR signaling. These observations identify another distinguishing feature between mice and humans in the TLR system that is likely to be due to differences in the selective pressure imposed by pathogens on each species during evolution.

The Toll-like receptors (TLRs)[1] are a family of molecules tailored to respond to microbial pathogens, with particular TLRs able to recognize and bind to specific pathogen-associated molecular patterns. Once activated, TLRs recruit cytoplasmic adapter molecules such as myeloid differentiation factor 88 (MyD88), MyD88 adaptor-like protein (Mal; also known as TIRAP), TIR domain-containing adaptor protein inducing interferon-β (TRIF; also termed TICAM-1), and TRIF-related adaptor molecule (TRAM; also termed TIRP or TICAM-2), which, in turn, initiate signaling cascades that result in biological responses geared toward the elimination of pathogens during infection (reviewed in Refs. 1 and 2).

Critical to the TLR signaling cascade are the interleukin-1 receptor-associated kinases (IRAKs). The first human IRAK to be cloned was IRAK1 (3), followed by IRAK2 (4), IRAK-M (5), and IRAK4 (6). The IRAKs share sequence homology to the *Drosophila melanogaster* protein kinase Pelle, and all contain a death domain (DD), which is used for protein-protein interactions with the DDs of other molecules. For example, IRAK2 uses its DD to mediate its interaction with MyD88 (4). The IRAKs also have putative kinase domains, although IRAK1 has dispensable kinase activity because interleukin-1-induced NF-κB activation could still be driven by a kinase-inactive mutant (7). In addition, both IRAK2 and IRAK-M are catalytically inactive due to the absence of certain key residues within their putative kinase domains (4–5).

Adding further complexity to the signaling cascades initiated by the TLRs are the recent findings that some of the genes encoding components of TLR signaling are alternatively spliced, thus generating multiple isoforms. One example is the murine *MyD88* gene, which encodes a full-length MyD88 ($MyD88_L$) and a shorter form ($MyD88_S$) generated by the splicing out of exon 3; the removal of this exon causes the deletion in the mature polypeptide of the intermediate domain (8). Both forms of MyD88 are differentially expressed and exhibit differences in their ability to induce NF-κB activation and IRAK phosphorylation, with $MyD88_S$ being inhibitory (8). $MyD88_S$ can, however, mediate the activation of c-Jun N-terminal kinase (9). Another example is the human *IRAK1* gene, which encodes two isoforms generated by the differential usage of a splice acceptor site within exon 12 (10). In contrast to the full-length isoform (designated IRAK1a), the slightly shorter isoform (IRAK1b) is kinase-inactive and displays no change in its protein levels following interleukin-1 stimulation (10).

Here, we report the identification and annotation of the murine *Irak2* gene, which generates four alternatively spliced isoforms of Irak2 that contain various deletions of the N-terminal third of the mature protein. Of these, Irak2a and Irak2b enhance the activity of an NF-κB reporter, whereas Irak2c and Irak2d are inhibitory. Our results therefore reveal a level of control of TLR signaling that involves differential splicing of murine *Irak2*.

EXPERIMENTAL PROCEDURES

Sequence Analysis—The complete nucleotide sequence of the murine *Irak2* gene and flanking regions was obtained from the National Center for Biotechnology Information (NCBI) mouse genomic data base (contig NT_039353 found at www.ncbi.nlm.nih.gov), following BLAST analysis with the human *IRAK2* cDNA (GenBank™ accession number AF026273). Other sequences used in this manuscript that were also obtained from the GenBank™ were the human *IRAK2* genomic locus (contig NT_005927) and *Irak2* cDNA (accession number AJ440756).

* This work was supported by Science Foundation Ireland. The costs of publication of this article were defrayed in part by the payment of page charges. This article must therefore be hereby marked "*advertisement*" in accordance with 18 U.S.C. Section 1734 solely to indicate this fact.

The nucleotide sequence(s) reported in this paper has been submitted to the GenBank™/EBI Data Bank with accession number(s) AY162378, AY162379, AY162380, and AY162381.

‡ To whom correspondence should be addressed: Dept. of Biochemistry and Biotechnology Inst., Trinity College Dublin, University of Dublin, College Green, Dublin 2, Ireland. Tel.: 353-1-608-2439; Fax: 353-1-677-2400; E-mail: laoneill@tcd.ie.

[1] The abbreviations used are: TLR, Toll-like receptor; aa, amino acid(s); DD, death domain; IRAK, interleukin-1 receptor-associated kinase; LPS, lipopolysaccharide; MEF, murine embryonic fibroblast; MyD88, myeloid differentiation factor 88; nt, nucleotide(s); RACE, rapid amplification of cDNA ends; RT, reverse transcriptase; UTR, untranslated region.

Transcription factor binding site searches were performed using TFSEARCH (molsun1.cbrc.aist.go.jp/research/db/TFSEARCH.html) (11) and MatInspector Release Professional (genomatix.gsf.de/mat_fam) (12). Global alignment of the human and mouse genomic sequences of conserved synteny was performed with the program AVID[2] using a window size of 100 bp and a conservation level of 70%; the results were viewed with the program VISTA (www-gsd.lbl.gov/vista/) (13–15). The identification of transcribed nucleotide sequences and repeat sequences in the genomic sequence was performed using the NIX application (hgmp.mrc.ac.uk). The translation of putative open reading frames was carried out using MacVector version 7.1 Oxford Molecular Ltd, and amino acid alignments were performed using ClustalW 1.8 (searchlauncher.bcm.tmc.edu). Domain predictions were determined using PROSITE (www.expasy.ch/prosite/) (16).

5′- and 3′-SMART™ Rapid Amplification of cDNA Ends (RACE)—5′- and 3′-SMART™ RACE-ready cDNA libraries were generated with or without reverse transcriptase according to the manufacturer's recommendations (Clontech) using 1 μg of polyadenylated (poly(A)$^+$) mRNA from normal C57Bl/6 murine embryonic fibroblasts (MEFs), thymus, placenta, or liver (Clontech) or from 1 μg of total human placental or spleen mRNA (Clontech). 5′- and 3′-RACE reactions were carried out according to the manufacturer's recommendations (Clontech) using 100 units of Advantage 2 polymerase, 0.2 pmol of universal primer mix, and 0.2 pmol of gene-specific primer (Table I) in a final volume of 50 μl. PCRs were amplified as described previously (17). To obtain specific RACE products, primary RACE PCR products were diluted 1:50 with 10 mM Tris-EDTA buffer and further amplified with Advantage 2 polymerase using 0.2 pmol of Nested universal primer (Clontech) and 0.2 pmol of Nested gene-specific primer (Table I) under conditions described previously (17). PCR products were analyzed by agarose gel electrophoresis and transferred to GeneScreen Plus nylon membranes, and their specificity was determined by hybridization with an internal oligonucleotide. Positive RACE PCR products were gel-purified, cloned into pGEM-T (Promega, Madison, WI), and sequenced.

Cell Culture and Reagents—Murine 3T3 fibroblasts and RAW264.7 cells were grown in RPMI 1640 medium (Sigma) supplemented with 10% fetal calf serum, 1% penicillin/streptomycin, and 1% L-glutamine (Sigma). The human embryonic kidney HEK293 cell line stably transfected with TLR4 (HEK293-TLR4) was a gift from Dr. Katherine Fitzgerald (University of Massachusetts Medical School) and was grown in Dulbecco's modified Eagle's medium (Sigma) supplemented as above with the addition of 600 μg/ml G418 (Sigma). Lipopolysaccharide (LPS) from *Escherichia coli* serotype O26:B6 was obtained from Sigma and used at 1 μg/ml. The pRL-TK vector was obtained from Promega, and the pCDNA3.0 vector was from Invitrogen (Carlsbad, CA) The pGL3-NF-κB construct bearing five repeats of the κB-consensus was a gift from Dr. R. Hofmeister (Universitaet Regensburg, Regensburg Germany). The human pCDNA-IRAK2 construct was obtained from Dr. Marta Muzio (Mario Negri Institute, Milan, Italy).

Reverse Transcriptase Polymerase Chain Reaction (RT-PCR)—Total RNA was extracted from 5×10^6 RAW264.7 cells treated with 1 μg/ml LPS for 0, 1, 3, 6, 9, and 24 h using TRI REAGENT™ according to the manufacturer's recommendations (Sigma). To each 10-cm^2 dish of LPS-treated cells was added 1 ml of TRI-REAGENT™, and the homogenous lysates were then centrifuged at 12,000 × *g* for 10 min. Each supernatant was added to 0.2 ml of chloroform and incubated at room temperature for 15 min following vigorous mixing. The RNA phase was then separated by centrifugation at 12,000 × *g* for 15 min, added to 0.5 ml of isopropanol, mixed, allowed to stand for 10 min then further centrifuged at 12,000 × *g* for 10 min. The RNA pellets were then washed with 1 ml of 70% ethanol and resuspended in 50 μl of H_2O. cDNA was generated from total RNA using Superscript™ III reverse transcriptase according to the manufacturer's recommendations (Invitrogen). To 9 μl of H_2O was added 1 μl 50 μM oligo(dT)$_{20}$ (Promega), 1 μg of total RNA, 1 μl of 10 mM dNTP, and the mixture was incubated at 65 °C for 5 min and then on ice for a further 5 min. To this mixture was then added 4 μl of 5× first-strand buffer (Invitrogen), 1 μl of 0.1 M dithiothreitol (Invitrogen), 1 μl of RNase inhibitor (1 unit/μl; Promega), and 1 μl of 200 units/μl Superscript™ III reverse transcriptase (Invitrogen) for plus RT libraries or 1 μl of H_2O for minus RT libraries; the final mixture was incubated at 50 °C for 60 min and then inactivated at 70 °C for 15 min. RT-PCR from RACE-ready cDNA libraries was performed on a PerkinElmer Life Sciences 2400 thermocycler in a reaction involving 2.5 μl 10× Vent (Roche Applied Science), 0.5 μl of Vent polymerase (2 units/μl; Roche Applied Science), 1 μl 10 mM dNTP, 10 μM each forward and reverse primer (MWG-Biotech; Table I), 2 μl of cDNA (plus or minus RT), and 17 μl of H_2O. PCR cycling conditions were 95 °C for 1 min and then 30 cycles at 95 °C for 1 min, 64–68 °C for 1 min, and 72 °C for 3 min. Amplified fragments were then cloned into pGEM-T and sequenced. For reverse transcribed cDNAs generated from LPS-treated RAW264.7 cells, the following reaction was used involving 2.5 μl of 10× Taq buffer (Promega), 3 μl of 25 mM $MgCl_2$ (Promega), 1 μl of 2.5 mM dNTP, 1 μl of 10 μM each forward and reverse primers (Table I), cDNA (plus or minus RT), 0.175 μl of Taq (5 units/μl; Promega) and 14.325 μl of H_2O. PCR cycling conditions for these reactions were 94 °C for 30 s and then 35 cycles at 94 °C for 10 s, 67 °C for 10 s, and 72 °C for 30 s followed by a final extension at 72 °C for 2 min. For glyceraldehyde-3-phosphate dehydrogenase gene RT-PCR, identical conditions were used except for an annealing temperature of 55 °C and 25 cycles instead of 35.

Northern Blotting—Northern blots were carried out using a murine eight-tissue blot (Clontech) according to the manufacturer's recommendations. Blots were hybridized at 68 °C for 90 min with a 1038-bp ^{32}P-labeled *Irak2* cDNA fragment (nucleotides (nt) 482-1527) corresponding to exons 4–11 inclusive of the *Irak2* gene. Blots were then washed at 50 °C with 0.2× SSC 0.1% SDS and exposed to Kodak X-OMAT film for 2 days at −70 °C.

Generation of Irak2 Expression Constructs—The entire open reading fames of *Irak2a*, *Irak2b*, *Irak2c*, and *Irak2d* were amplified by PCR from a murine liver cDNA library (Clontech) using the primers Irak2-14 (for *Irak2a*, *2b*, and *2d*), Irak2-15 (for *Irak2c*), and Irak2-16 as a common reverse primer (Table I). PCR was carried out on a PerkinElmer Life Sciences 2400 thermocycler using the following conditions: 2.5 μl 10× Vent; 1 μl of 10 mM dNTP; 0.5 μl of Vent polymerase (2 units/μl); 1 μl of 20 ng/μl cDNA; 1 μl each of 10 μM 5′ and 3′ primers (Table I), and 18 μl of H_2O. The following cycling conditions were then used: 95 °C for 1 min; 35 cycles at 95 °C for 1 min; 68 °C for 1 min; and 72 °C for 3 min. All *Irak2* constructs were generated to encode in-frame hemagglutinin A tags (YPYDVPDYA) at their C termini using the primer Irak2-17 and contained BamHI and EcoRI linkers at their 5′- and 3′-ends, respectively; these linkers were subsequently cleaved with their respective restriction endonucleases (New England Biolabs, Hertfordshire, UK), subcloned into pCDNA3.0, and sequenced.

Transient Transfection—Cells were seeded at ~1×10^5 cells/ml into 24-well plates in complete growth media and cultured at 37 °C (in the presence of 5% CO_2) until 50–80% confluent. To 17 μl of serum-free media was added 3 μl of GeneJuice™ (Novagen, La Jolla, CA); following mixing and a 5 min incubation at RT, the solution was added to 450 ng of plasmid DNA, gently mixed, incubated for a further 15 min at RT, then added dropwise to each well of the 24-well plate. This was performed in triplicate for each assay point. The composition of the transfected DNA typically consisted of 100 ng of *Renilla* luciferase (pRL-TK), 200 ng of NF-κB-luciferase reporter, and 25–150 ng of Irak2 expression plasmids, and the remainder was empty vector (pCDNA3.0) up to 150 ng. Following transfection, cells were either left untreated at 37 °C (5% CO_2) for 24 h or treated with LPS at 1 μg/ml for 16 h. Optimal treatment times had been determined previously by time course, and total incubation time for all transfected cells was 24 h. Cells were then lysed in 300 μl/well of 1× passive lysis buffer (Promega) for 15 min at room temperature, and 30 μl each of the lysate was analyzed in duplicate for firefly luciferase and *Renilla* luciferase activity using a Mediators PhL luminometer. Reporter activity was then determined as a function of firefly luciferase activity divided by the *Renilla* luciferase activity. Differences between means were calculated using Student's *t* test analysis.

RESULTS

Identification of the Murine Irak2 Gene—To identify the murine orthologue of the human *IRAK2* gene, a BLAST search of the murine genomic DNA data base using the human *IRAK2* cDNA sequence of Muzio *et al.* (4) was performed. A region of significant homology was found on *Mus musculus* (MMU) chromosome 6 at position E3. This putative *Irak* gene was not murine *Irak1*, *Irak4*, or *Irak-M*, because these genes lay on other chromosomes; this gene was therefore likely to be *Irak2*. To obtain a complete annotation of the putative *Irak2* gene, ~120-kb pairs of murine genomic DNA encompassing this gene was analyzed in detail using the NIX suite of programs, which are able to identify putative exons, transcriptional units, polyadenylation signal sequences, CpG islands, and repetitive ele-

[2] N. Bray, A. Fabrikant, J. Lord, J. Schwartz, I. Dubchak, and L. Pachter, unpublished work.

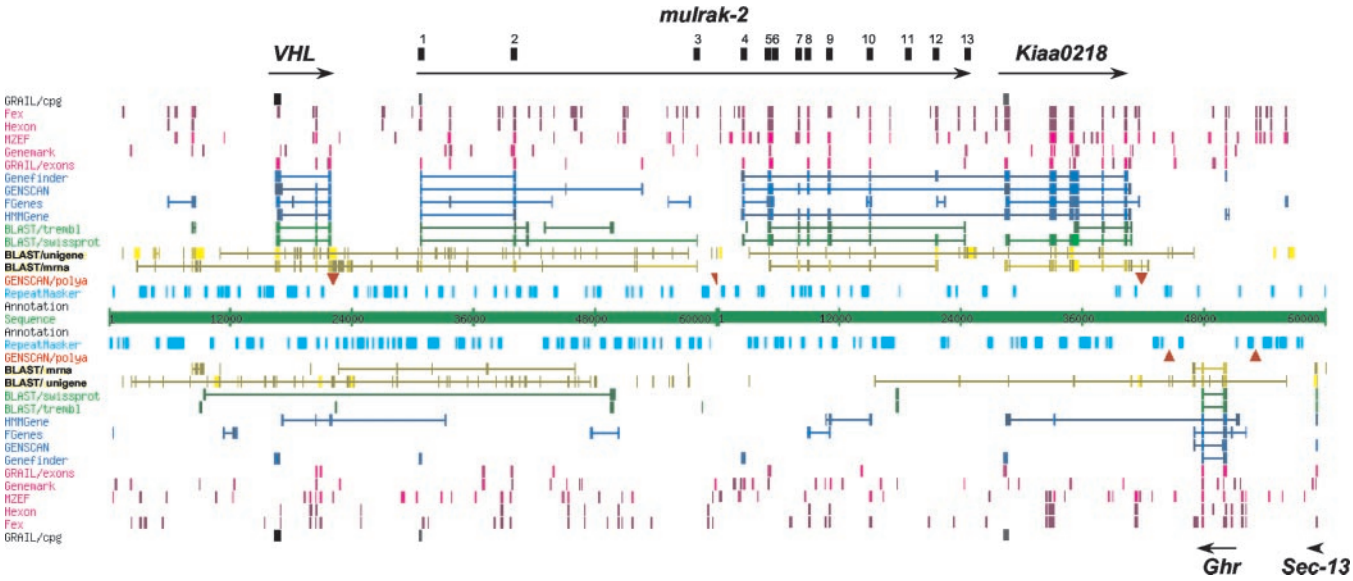

FIG. 1. **NIX nucleotide identity analysis of the murine genomic region encoding the murine *Irak2* gene.** The following programs within the NIX suite were used to identify transcriptional units: GRAIL/cpg (identifies putative GC-rich regions that often overlap first exons); Fex, Hexon, MZEF, Genemark, and GRAIL/exons (programs that identify putative exons); Genefinder, GENSCAN, Fgenes, and HMMGene (predict putative genes); BLAST/trembl and BLAST/swissprot (BLAST of putative open reading frames against protein databases); BLAST/unigene and BLAST/mrna (performs BLAST analyses against mRNA/gene databases); GENSCAN/polya (identifies putative polyadenylation signal sequences); and RepeatMasker (masks repetitive elements). Outputs above the *central horizontal bar* are analyses on the sense strand; those below the bar are those on the antisense strand. *Arrows* and *names* indicate the predicted genes and their direction of transcription. The individual exons encoded by the *Irak2* gene are shown by *black boxes* and are numbered.

ments within the genomic sequence to be analyzed. As shown in Fig. 1, the NIX programs were able to readily identify the murine *Irak2* gene and the positions of the majority of the individual exons of the *Irak2* gene with the exception of exons 3 and 11. This prediction was confirmed by BLASTN and BLASTX analysis and alignment of the *huIRAK2* cDNA sequence against the murine genomic sequence. The putative *Irak2* gene encompasses ~55 kb of murine genomic sequence and is transcribed toward the center of *MMU* chromosome 6 (Fig. 1). ~7 kb 5′ of the putative exon 1 of *Irak2* lies the well predicted murine Von Hippel-Lindau disease tumor suppressor gene (*VHL*; GenBank™ accession number P40338), a multiexon gene of ~6-kb transcribed in the same orientation as *Irak2* (Fig. 1). Immediately 3′ of *Irak2* lay another predicted gene with the designation *Kiaa0218* (Fig. 1) with strong homology to human *KIAA0218*, a gene encoding a putative deoxyribonuclease (GenBank™ accession number Q93075). This murine transcriptional unit also appears to be transcribed in the same orientation as *VHL* and *Irak2*. The human homologues of all three murine genes are found in exactly the same positions on *Homo sapiens* chromosome 3p25.3, transcribed toward the centromere (data not shown). Located further 3′ of murine *Kiaa0218*, transcribed in the opposite orientation, was a putative transcriptional unit (the *Ghr* gene) encoding the murine Ghrelin precursor (also known as the growth hormone secretagogue, the growth hormone-releasing peptide, the motilin-related peptide, and the M46 protein; GenBank™ accession no. Q9EQX0) (Fig. 1).

Identification of Multiple Irak2 cDNAs—To obtain *Irak2* cDNA sequence information, primers were designed (Irak2-1 and Irak2-2; Table I) within two regions of murine genomic sequence with high homology to the human *IRAK2* cDNA; these primers were also located at either end of the putative gene (exons 2 and 12) to amplify as much cDNA as possible. Surprisingly, RT-PCR amplification from a MEF cDNA using these primers library yielded two fragments of ~1200 and 1350 bp (Fig. 2*A*), which strongly suggested differential splicing of the murine *Irak2* gene. No products were amplified from minus RT MEF cDNA, demonstrating that these products were not the result of genomic DNA contamination (data not shown). Upon sequencing of these PCR products, it was determined that the larger cDNA fragment (designated *Irak2a*) was encoded by exons 2–12, inclusive, of the putative *Irak2* gene. The amplified cDNA sequence also matched the predicted exons, thus providing confirmation of the efficacy of the prediction programs used. The smaller cDNA fragment lacked a sequence encoded by exon 3 but was otherwise identical to the larger amplified cDNA; this cDNA therefore appeared to be a variant of *Irak2* (we have designated this cDNA *Irak2b*).

To further annotate the genomic structure of *Irak2*, identify its 5′ and 3′ ends, and identify additional *Irak2* variants, RACE PCR was performed using murine thymus, placenta, liver, and MEF RACE cDNA libraries, with similar results obtained. 5′-RACE and nested 5′-RACE PCR was first performed using primers located in exons 6 and 5, respectively (Irak2-3 and Irak2-4; Table I). Two products of ~650 and 500 bp were amplified (Fig. 2*B*); the larger fragment, when sequenced, corresponded to *Irak2a*, and the smaller fragment corresponded to the exon 3-deficient *Irak2b*. A smaller PCR product of ~400 bp was also observed (Fig 2*B*); upon sequencing, this product turned out to be nonspecific. 5′-RACE also identified the putative exon 1 and two distinct 5′ terminations at positions 1 and 33 of the *Irak2a* cDNA. Also identified by 5′-RACE were several 650- and 500-bp clones (Fig. 2*B*) that generated further variant *Irak2* cDNA sequences. Several of the 650-bp cDNA fragments generated utilized the 3′ 420 bp of intron 3 before reading directly into exon 4; we designated this isoform *Irak2c*. Several 500-bp cDNA fragments were also found to contain an *Irak2* cDNA sequence similar to that of *Irak2a* but lacking a sequence encoded by exon 2; this isoform has been designated *Irak2d*.

To confirm the existence of the *Irak2c* and *Irak2d* cDNAs, RT-PCR was performed using a MEF cDNA library (Fig. 2*C*) and isoform-specific primers (Irak2–5 and Irak-6 for *Irak2c*; Irak2–7 and Irak-6 for *Irak2d*). The *Irak2c* and *Irak2d* RT-PCR reactions generated 400- and 510-bp PCR products, respec-

TABLE I
Oligonucleotides used

Name	Sequence (5′ → 3′)	Usage
Irak2-1	5′-TGGACCTCCTGTGTCACCTGGAACTCT-3′	RT-PCR
Irak2-2	5′-CAACGTCATCTGTTTCCTCCGGGGTAT-3′	RT-PCR
Irak2-3	5′-GCTGCATCTCTGCCTGTAGGAATCTGTCCA-3′	5′-RACE
Irak2-4	5′-GCTTGGACGACATCTGCTTCACTCCAGAAA-3′	5′-RACE
Irak2-5	5′-CTTCGGGATGCGTCCCCAGGCAGA-3′	RT-PCR
Irak2-6	5′-GCTGCATCTCTGCCTGTAGGAATCTGTCCA-3′	RT-PCR
Irak2-7	5′-ACTGGATGCAGTTCGGGAAGCCGGTTC-3′	RT-PCR
Irak2-8	5′-CCATGGCTTGCTACATCTACCAGCTGCCGT-3′	RT-PCR
Irak2-9	5′-CATCAGGGTCCAAAGAGCTCGCTGCTGTCC-3′	RT-PCR
Irak2-10	5′-CTTCAGTCTGCTCCAGGAAGACCAGCA-3′	3′-RACE
Irak2-11	5′-GTTTCTGAGGCCACAGGCTCATCTTCCAAT-3′	3′ -RACE
Irak2-12	5′-GGCCCATCATGGCTGGGGCCCAGCGGCAGC-3′	Northern blot
Irak2-13	5′-CTCCTCCACGCTGGCATTGCGCCTCCGCAG-3′	Northern blot
Irak2-14	5′-GCGGATCCATGGCTTGCTACATCTACCAGC-3′	Constructs
Irak2-15	5′-CTGGATCCATGGCTGGGGCCCAGCGGCAGC-3′	Constructs
Irak2-16	5′-GTCGGGAACGTCGTAGGGGTAGGGTCCAAAGAGCTCGCT-3′	Constructs
Irak2-17	5′-GCGGAATTCCTAGGCGTAGTCGGGAACGTC-3′	Constructs
Irak2-18	5′-AGATTGTCTTGAGCTGGAAGCCGGTTCCTG-3′	RT-PCR
HuI2-1	5′-TTCCTGCTTAGGAATGGAGGTGCTGAAGTC-3′	5′-RACE
HuI2-2	5′-AAGTGGGGAGGTCGCTTCTCAAGGAATGAG-3′	5′-RACE
HuI2–3	5′-CTGCTACATCTACCAGCTGCCCTCCTG-3′	RT-PCR
huI2-4	5′-CAACACAGGCCTCAGAGGAGGAGTCAG-3′	RT-PCR
GAPDH-F[a]	5′-GAACGGGAAGCTTGTCATCAA-3′	RT-PCR
GAPDH-R[b]	5′-CTAAGCAGTTGGTGGTGCAG-3′	RT-PCR

[a] Glyceraldehyde-3-phosphate dehydrogenase (forward).
[b] Glyceraldehyde-3-phosphate dehydrogenase (reverse).

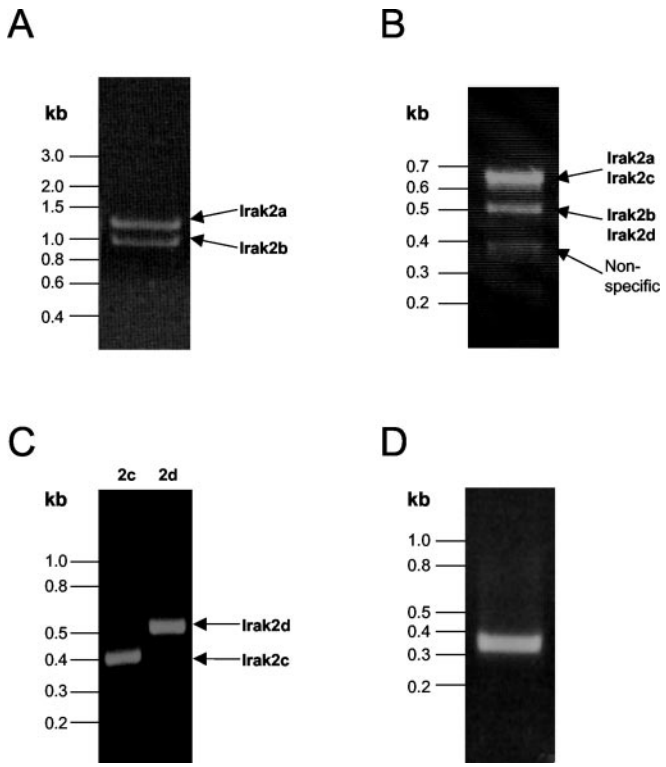

FIG. 2. **Identification of multiple *Irak2* cDNAs.** *A*, RT-PCR of murine Irak2a and Irak2b cDNAs from a MEF cDNA library using gene-specific primers. *Arrows* indicating the identity of each band are shown. *B*, 5′-RACE analysis from a MEF RACE cDNA library using gene-specific primers. Similar results were also obtained using thymus, placental, and liver cDNA libraries. The identity of each band is also shown. *C*, RT-PCR of Irak2c and Irak2d using gene-specific primers and a MEF cDNA library. *D*, 3′-RACE analysis using a murine liver cDNA library and gene-specific primers.

tively; these were sequenced and the results confirmed the presence of these isoforms. As final confirmation, the open reading frames of all putative *Irak2* isoforms were amplified by RT-PCR using Irak2–8 and Irak2–9 primers for *Irak2a*, *2b* and *2d* cDNAs, and Irak2–5 (exon 4′) and Irak2–9 for *Irak2c* (Data not shown). The *Irak2a* is the same cDNA as that previously described (18). Amplification of the *Irak2d* cDNA also revealed a 30-nt deletion in exon 12 in addition to the deleted exon 2 (data not shown). For all RT-PCR reactions, no PCR products were generated using a minus RT MEF cDNA library (data not shown). To locate the 3′-end of the *Irak2* gene, 3′-RACE was performed using the Irak2–10 and Irak2–11 primers located in exons 11 and 12, respectively (Table I). A single PCR fragment of ~350-bp was generated (Fig. 2*D*), which, upon sequencing, was found to contain an *Irak2* cDNA sequence encoding exons 12 and 13. All four *Irak2* cDNA sequences were confirmed against the murine genomic sequence data base by BLASTN and BLASTX and have been deposited into GenBank™ under the accession numbers AY162378, AY162379, AY162380, and AY162381.

Gene Structure and Alternative Splicing of Murine Irak2—The murine *Irak2* gene is composed of 13 exons and 12 introns and encodes a predicted full-length protein of 622 amino acids (aa) (Fig. 3*A* and Table II). Full-length Irak2 contains a well predicted kinase domain (aa 206–471) and a weakly predicted DD (aa 14–93). Exon 1 contains the common 5′-untranslated region (UTR) of *Irak2a, 2b*, and *2d*, as well as their common initiating codon (ATG), and also encodes the N terminus (aa 1–13). Exon 2 encodes the entire DD; exons 3 and 4 encode what we now designate as the α and β subdomains of the interdomain (aa 94–205), respectively; exons 5–11 encode the kinase domain; exons 12 and 13 encode the C terminus (aa 472–622); and the termination codon for all *Irak2* variants lies in exon 13 (Fig. 3*A*). *Irak2c* has its own 5′-UTR (designated exon 4′) that is encoded by a 5′ continuation of exon 4. Intron sizes range from 83 bp (intron 5) to almost 18 kb (intron 2), and the intron-exon boundaries of *Irak2* conform to the GT-AG rule (Fig. 3*A*) (19) (Table II). The three possible codon disruption phases are present in the *Irak2* gene splice junctions; introns 4, 5, 7, 9, 10, and 11 disrupt exons between amino acids (phase 0), introns 1, 2, and 3 interrupt a codon between the first and second nucleotide (phase 1), and introns 6 and 8 disrupt a codon between the second and third nucleotide (phase 2) (Table II).

The alternative splicing of *Irak2* isoforms is shown in detail in Fig. 3*B*. *Irak2a* utilizes every exon consecutively. However,

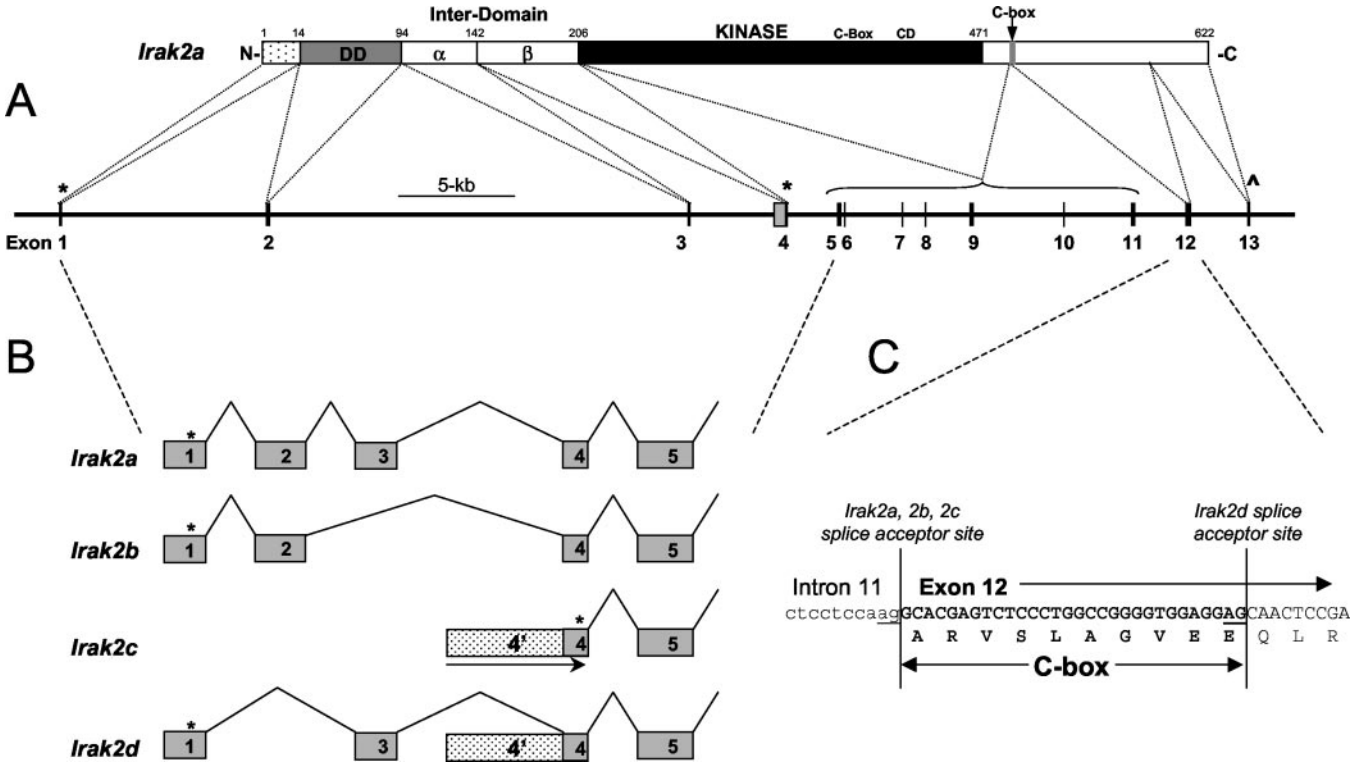

FIG. 3. **Alternative splicing of the murine *Irak2* gene.** *A*, a schematic representation of the genomic structure of *Irak2*. Exons (*numbered black boxes*) are shown on the genomic sequence (*horizontal line*) with start and stop codons indicated by *asterisks* (*) and *carets* (^), respectively. The mature Irak2a protein is represented above with the N terminus (*dotted box*), the death domain (*gray box*), the interdomain, the kinase domain (*black box*), and C terminus shown. Numbers above the bar indicate the amino acid start points of each putative domain. *B*, alternative splicing patterns at the 5′-end of *Irak2* that lead to the formation of multiple Irak2 isoforms. *Irak2a* utilizes all 5′-exons; *Irak2b* and *Irak2d* are generated by exon skipping of exons 3 and 2, respectively, and *Irak2c* has its own 5′-UTR (designated exon 4′; *dotted box*). Start codons used by each isoform are indicated by *asterisks*. *C*, detail of the intron 11/exon 12 boundary, showing the differential splice acceptor sites (*underlined*) used by the *Irak2* isoforms. Intronic sequences are in *lowercase letters*; exonic sequences are in *uppercase letters*. The sequence encoding the putative C-box is highlighted in *boldfaced type*. Below the nucleotide sequence is the translated sequence shown in single letter format.

TABLE II
Intron-exon boundaries of the murine Irak2 gene

The differential splice acceptor sites are set in boldfaced type. Intronic sequences are in lowercase letters, and exonic sequences are in uppercase letters.

3′ Splice acceptor site	Exon	Base pairs	5′ Splice acceptor site	Intron	Base pairs	Splice phase
	1	154	GGATGCAGTTCG**gt**gagtgaca W M Q F	1	9,036	1
tgccttcc**ag**CTTCCTACGTGA A S Y V	2	183	TTGTCTTGAGCT**gt**gagtaact I V L S	2	17,880	1
cttgttcc**ag**GGAAGCCGGTTC W K P V	3	144	TTCTAGACACAG**gt**gctctcct L L D T	3	4,352	1
tcctttct**ag**GGCCCATCATGG G P I M	4	95	CCCCAGTCTAAG**gt**aaatccac P Q S K	4	2,445	0
caatctcc**ag**TATTGCAGTACT Y C S T	5	201	AAGCTCAGGGAG**gt**gaggtgag K L R E	5	83	0
tttcccac**ag**GTGGCCGGCTCC V A G S	6	65	GCTCTGCCTCAG**gt**aagcttcc L C L R	6	2,543	2
ctgggttc**ag**ATGCTGCCACGC C C H A	7	115	CTCTGGGCTCAG**gt**aaaccagt L W A Q	7	844	0
tttctctt**ag**GGCAACTCAGAC G N S D	8	110	CAATGTTAAGAG**gt**gagagggc N V K S	8	1,950	2
tttcccgc**ag**TGCCAACGTCTT A N V L	9	196	AGCTGTGGAATT**gt**aagcattt S C G I	9	3,888	0
tcctaccc**ag**GTATTGGCCGAG V L A E	10	63	CCAGTTTACCTG**gt**aagagatc P V Y L	10	3,830	0
cttcccat**ag**AAGGATTTGCTT K D L L	11	201	AGCGTGGAGGAG**gt**gagctctc S V E E	11	2,359	0
ctcctcca**ag**GCACGAGTCTCC A R V S	12	290	CACCCCAGAACG**gt**aagcttgg	12	2,609	
tgaacatc**ag**CTACAGAGACTT	13	131				

Irak2b and *Irak2d* are generated by the deletion of exons 3 and 2, respectively, in a process called exon skipping. *Irak2d* also utilizes an alternative splice acceptor site 30 bp into exon 12, which causes the deletion of 10 amino acids (designated the C-box) in the C terminus (Fig. 3*D*). The function of the C-box (ARVSLAGVEE) is unknown, and no matches to any known

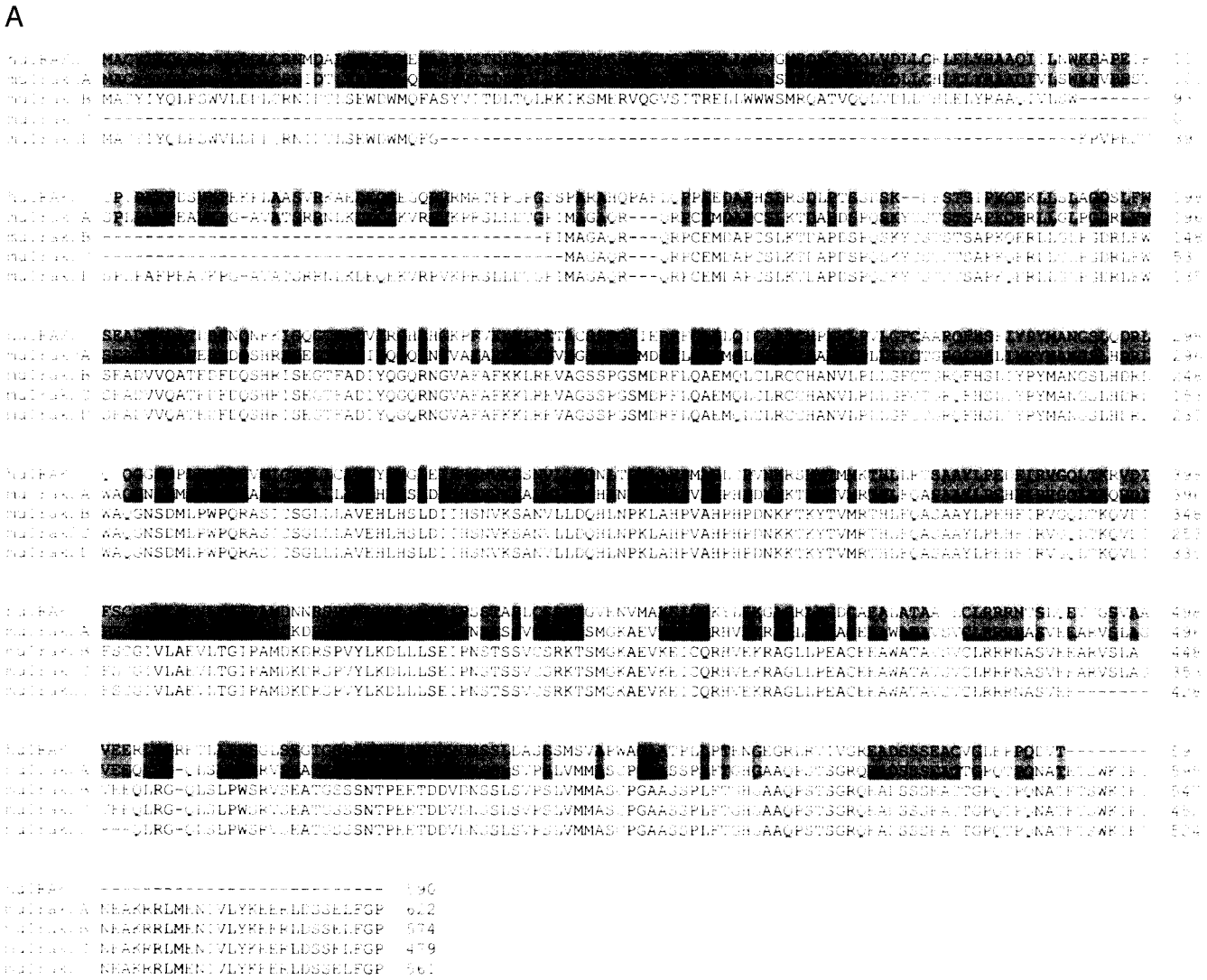

FIG. 4. **Comparative analysis of human IRAK2 and murine Irak2.** *A*, ClustalW alignment of the human IRAK2 amino acid sequence with the putative amino acid sequences of the murine Irak2 isoforms. Regions of amino acid identity between IRAK2 and Irak2a are *shaded*. *B*, global alignment of the human *IRAK2* and murine *Irak2* genes along with the flanking genes *VHL* and *KIAA0218*. Numbers on each *y*-axis represent the percentage identity between humans and mice of nucleotides in a 100-bp window. Numbers on the *x*-axis indicate the nucleotide position from a position ~14 kb 5′ of the murine *Vhl* gene. Conserved regions in which the average identity is >75% are *shaded* below the curve. The *VHL* and *KIAA0218* genes are indicated by *dotted arrows*, and the *IRAK2* gene is indicated by a *solid arrow*. The *IRAK2* exons are also shown (*gray boxes*) below the *arrow*.

protein motifs were found. *Irak2c* is not generated by exon skipping, but has its own specific 5′-UTR in intron 3 (exon 4′); its ATG lies in exon 4. (Fig. 3*B*). Alternative splicing of *Irak2* therefore gives rise to natural truncation mutants of Irak2 as follows: Irak2a (a putative 622 amino acid protein) is full-length; Irak2b (574 amino acids) lacks the α subdomain of the interdomain; Irak2c (479 amino acids) lacks the N-terminal 143 amino acids; and Irak2d (561 amino acids) lacks the DD and the C-box.

Comparison of the nucleotide sequences of the full-length *Irak2a* cDNA described here and the *Irak2* cDNA isolated by Rosati and Martin (18) (GenBank™ accession number AJ440756) revealed several nucleotide differences occurring at nt 308 (P103L), nt 629 (R210Q), nt 668 (C223Y), nt 704 (R235K), nt 992 (R331H), nt 1048 (T350A), nt 1642 (T548A), and nt 1732 (A578T). However, there is no evidence of these nucleotides being polymorphic, as detailed comparisons of our generated cDNA sequences from multiple cDNA libraries with available genomic and expressed sequence tag (EST) sequences show total conservation. Taken together, these data suggested that the *Irak2* nucleotide sequence generated at these positions by Rosati and Martin (18) could be artifacts of the PCR amplification of their cDNA. There is a polymorphism in the *Irak2* cDNA that has been confirmed by the following: (i) sequencing of multiple cDNA clones generated here; (ii) a comparison with known cDNA sequences; and (iii) BLASTN and BLASTX analyses of genomic and expressed sequence tag databases. This polymorphism lies at nt 1343 in the cDNA of (18) and results in an E448V variation.

Comparative Analyses of Human IRAK2 and Murine Irak2—Because *Irak2* is an alternatively spliced gene, the possibility was raised that alternatively spliced *huIRAK2* isoforms may also exist. To determine their existance, we first aligned the putative amino acid sequences of IRAK2 and Irak2a. Human IRAK2 and murine Irak2a are well conserved (~65% amino acid identity), with their putative death and kinase domains particularly well conserved (93 and 75% amino acid identity, respectively) (Fig. 4*A*). This fact suggests that the functions of IRAK2 attributed to these domains may be shared in humans and mice. However, the interdomain and the C termini display a lower level of amino acid identity (51 and 41%, respectively) (Fig. 4*A*). The ATG used by Irak2c is also mutated to a proline

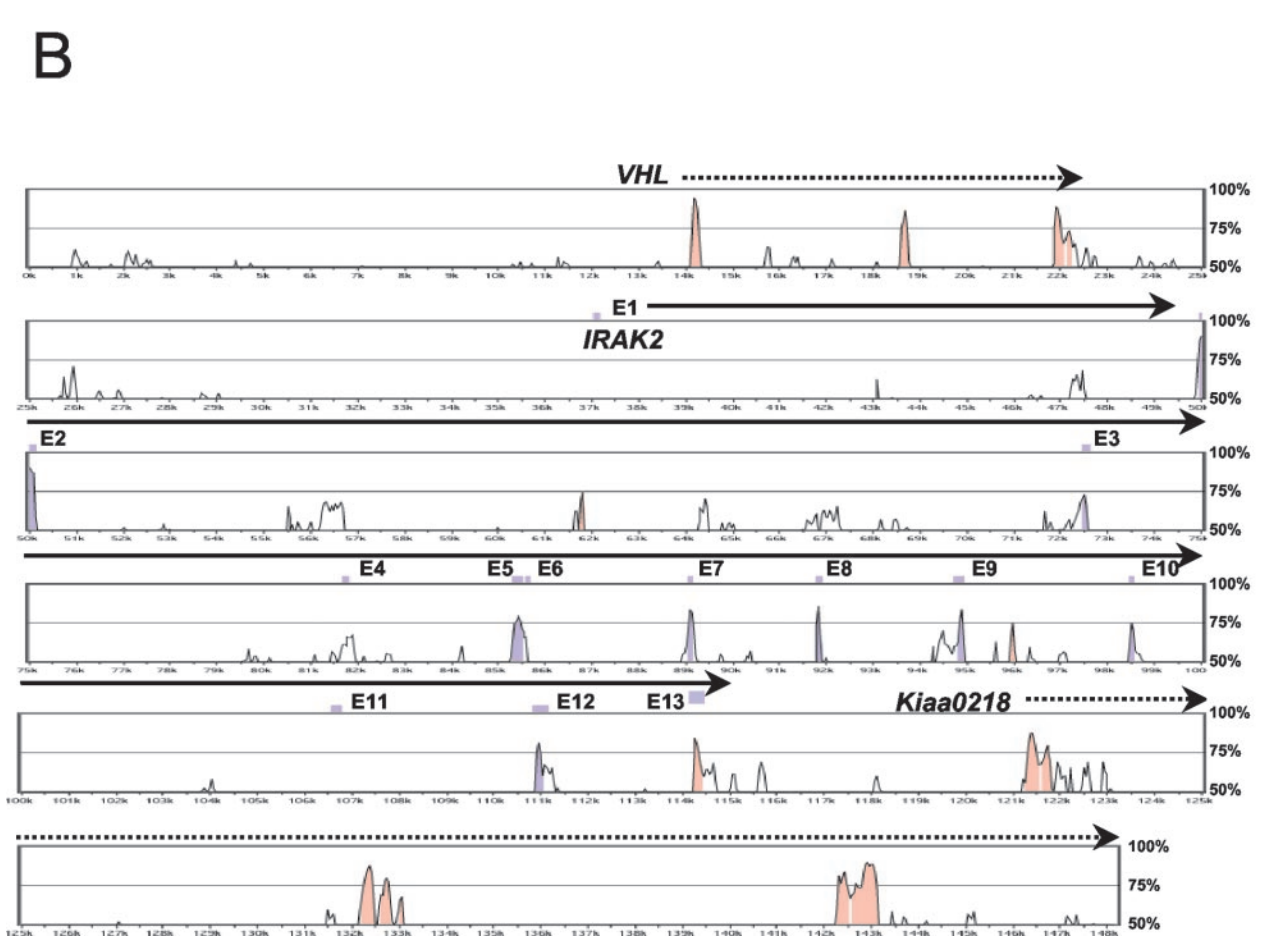

FIG. 4—*continued*

residue at the same position in IRAK2, suggesting that a similar IRAK2C orthologue does not exist.

We then performed 5′-RACE PCR using human spleen and placental RACE libraries and primers located in exon 5 (huI2-1) and exon 4 (huI-2) to try to identify possible human *IRAK2B* and *IRAK2D* cDNAs. A single RACE PCR product of ~550 bp was generated, cloned, and sequenced (data not shown). Only a match to the previously identified *IRAK2* cDNA of Muzio *et al.* (4) was found despite sequencing of more than 30 individual clones. To confirm the lack of alternative splicing of the *IRAK2* gene, RT-PCR was performed using primers corresponding to exons 1 and 12 (huI2-3 and huI2-4). A single PCR product of ~1.7 kb was generated, which was shown to be full-length *IRAK2* upon cloning and sequencing (data not shown). These data suggest that only one form of human IRAK2 exists, in contrast to the multiple Irak2 isoforms.

Comparisons of human and mouse coding and non-coding genomic sequences in regions of conserved synteny have previously been successful in identifying common elements regulating gene expression (20). To test this hypothesis, we aligned the human and mouse genomic regions containing and flanking the *IRAK2* genes and found that the coding sequences of the *IRAK2* and *Irak2* genes were generally well conserved (Fig. 4*B*). However, no conserved non-coding sequences were identified between humans and mice. These data suggest that IRAK2 and Irak2 may be differentially regulated despite sharing some core functional similarities mediated by their conserved death and kinase domains.

Analysis of Putative Murine Irak2 Promoter Elements—The 5′-UTR utilized by *Irak2a, 2b*, and *2d* and that utilized solely by *Irak2c* are separated by ~30 kb in the mouse genome (Fig. 1). This suggests that the expression and regulation of Irak2c occur though a different promoter to that of the other Irak2 isoforms. The 5′ sequence flanking exon 1 and exon 4′ of the *Irak2* gene were therefore analyzed for the presence of putative transcription factor binding sites that may give clues as to how this gene may regulate expression of Irak2 isoforms. Analysis of the putative *Irak2c* promoter 5′ of exon 4′ revealed multiple transcription factor binding sites for NF-κB (21–22), signal transducers and activators of transcription 1 (23), and interferon regulator factor 7 (24) as well as an interferon-stimulated response element (25) (data not shown). In contrast, the genomic sequence 5′ of exon 1 did not contain any of these putative binding sites, which suggests that Irak2c may be

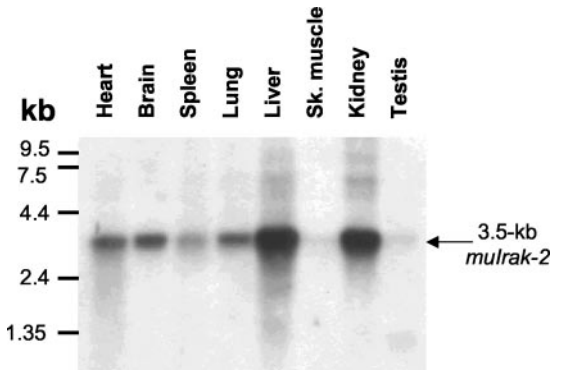

FIG. 5. **Expression of *Irak2* mRNA.** A Clontech eight-tissue poly $(A)^+$ mRNA blot was hybridized with a 1038-bp ^{32}P-labeled *Irak2* cDNA fragment corresponding to exons 4–11 inclusive of the *Irak2* gene.

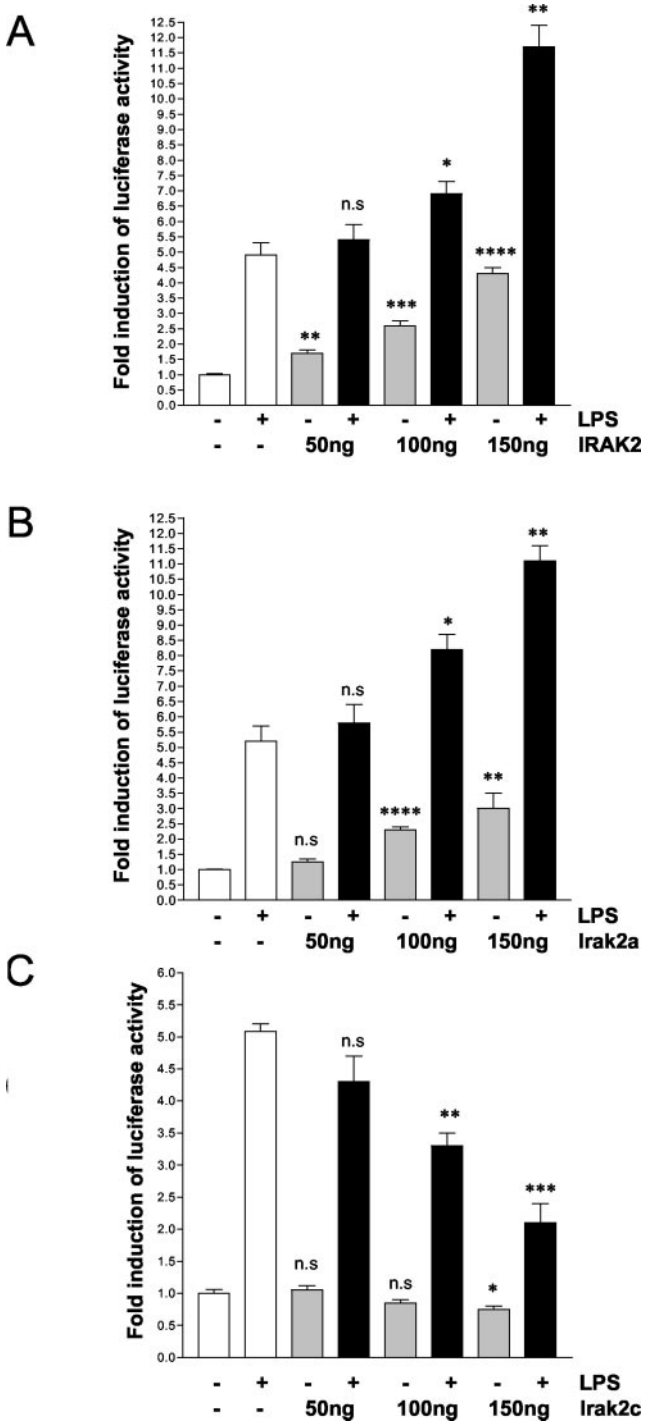

FIG. 6. **Role of Irak2 isoforms in LPS-mediated signaling.** Murine 3T3 cells were transfected with an NFκB-luciferase reporter gene with or without 50, 100, or 150 ng of expression constructs encoding human IRAK2 (*A*), murine Irak2a (*B*), and Irak2c (*C*). Transfected cells were then left untreated or treated with 1 μg/ml LPS for 16 h. Results are expressed as the mean ± S.E. ($n = 3$) fold increase in luciferase activity relative to unstimulated cells for each reporter tested and are representative of four separate experiments. Similar results were obtained using HEK293-TLR4 cells. p values were calculated using Student's t test analysis (*, $p < 0.05$; **, $p < 0.005$; ***, $p < 0.001$; ****, $p < 0.0005$; *n.s.*, not significant), comparing overexpressed Irak2 without LPS treatment (*gray histobars*) against ectopic NF-κB-luciferase or LPS-treated cells containing overexpressed Irak2 against LPS-induced NF-κB-luciferase activity.

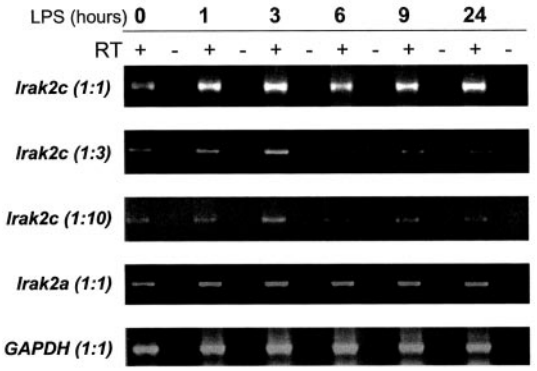

FIG. 7. **Regulation of Irak2 isoforms by LPS.** RT-PCR of murine *Irak2c* and *Irak2a* in RAW264.7 cells treated with 1 μg/ml LPS for 0, 1, 3, 6, 9, and 24 h. Gene-specific primers were used to amplify these cDNAs, which were either used neat or serially diluted 1:3 or 1:10. Minus RT and glyceraldehyde-3-phosphate dehydrogenase gene (*GAPDH*) controls are also shown.

regulated in response to stimuli such as LPS when compared with the other Irak2 isoforms.

Expression of Irak2—To obtain a representative expression profile of *Irak2*, we probed a mouse eight-tissue blot with a 1038-bp cDNA probe corresponding to exons 4–11 of the *Irak2* gene amplified from a MEF cDNA library by RT-PCR using the Irak2–12 and Irak2–13 primers (Table I). These exons are used by all *Irak2* isoforms, meaning that the resulting mRNA expression profile would be representative of *Irak2* as a whole. As shown in Fig. 5, we detected the presence of a single 3.5-kb mRNA transcript in all tissues tested, which is smaller than the 4.4-kb transcript reported previously (18). It is not surprising that only a single transcript was detected, given the similar sizes of the individual cDNAs of *Irak2* and the resolution level of the Northern blot itself. This transcript was dominant in liver and kidney and weak in testes and skeletal muscle. An additional transcript of 1.3 kb was also detected in testes; the identity and function of this transcript is unknown. Several minor transcripts were detected with mRNA mobilities of >6.5-kb (Fig. 5); these transcripts most likely represent nonspecific hybridization or unprocessed mRNA. The tissue-specific expression of *Irak2* mRNA was found to differ from that of human *IRAK2* mRNA, which was found to be most highly expressed in the lung, liver, skeletal muscle, and spleen (4), in contrast to the relatively weak expression of *Irak2* in murine lung, skeletal muscle, and spleen as compared with that in murine liver (Fig. 5). These data further suggest that IRAK2 and Irak2 may function differently *in vivo*, provided their protein expression correlates with their mRNA expression. We could not test for murine Irak2 protein expression because of the lack of availability of an Irak2-specific antibody.

Irak2 Isoforms Have Different Effects on Ectopic and LPS-induced NF-κB Activity—To assign putative functions to the Irak2 isoforms, we tested them for their ability to influence the activity of an NF-κB reporter gene either ectopically or upon stimulation with LPS. As shown in Fig. 6*A*, LPS was able to confer an increase in luciferase activity of ~5-fold in murine 3T3 fibroblasts as compared with untreated cells. Human IRAK2, when transiently transfected with the NF-κB reporter, was able to dose-dependently increase NF-κB-luciferase activity and potentiate the effect of LPS in this response (Fig. 6*A*). When an Irak2a expression construct was transfected into 3T3 cells (Fig. 6*B*), a similar effect was observed both on its own and on LPS-induced NF-κB-luciferase activity. When Irak2b was tested in the same assay, similar results were obtained (data not shown), suggesting that the removal of the α subdomain of the Irak2 interdomain has no effect on Irak2 activity. Interestingly, when an Irak2c expression construct was tested for its ability to influence NF-κB reporter activity in 3T3 cells (Fig.

6*C*), a dose-dependent inhibition of LPS-induced NF-κB activity was observed, suggesting that the N-terminal half of Irak2 that is absent in Irak2c mediates the downstream signaling mediated by LPS. Similar results were found with Irak2d (data not shown), confirming that the death domain of Irak2 is required for Irak2 function. None of the isoforms had an effect on cells transfected with pCDNA3.0 alone (data not shown). Taken together, these data suggest that the different isoforms of Irak2 have distinct functions, with Irak2c and Irak2d being inhibitory.

LPS Induces Irak2c Expression—Finally, we tested for the ability of murine Irak2 isoforms to be differentially regulated in response to LPS, because only the putative *Irak2c* promoter appeared to contain LPS response elements such as NF-κB. We used RT-PCR from cDNAs generated from LPS-treated RAW264.7 cells, as Northern blotting would not have been able to discriminate between Irak2 isoforms. As shown in Fig. 7, we were able to amplify a 399-bp *Irak2c*-specific cDNA fragment from RAW264.7 cells using the Irak2-5 and Irak2-6 primers (Table I). The levels of amplified *Irak2c* appear to increase relative to that of the glyceraldehyde-3-phosphate dehydrogenase gene following 1 and 3 h of LPS treatment before falling back toward pretreatment levels, suggesting that LPS may indeed regulate *Irak2c*. This apparent up-regulation of *Irak2c* was also observed when the cDNA used was serially diluted at 1:3 and 1:10 (Fig. 7), suggesting that this effect is not an artifact of the PCR cycling conditions. We were also able to amplify a 510-bp *Irak2a*-specific fragment (Fig. 7) using a forward primer spanning exons 2 and 3 (Irak2-18) and the reverse primer Irak2-6 (Table). However, the levels of *Irak2a* cDNA amplified did not appear to change following LPS treatment relative to those of the glyceraldehyde-3-phosphate dehydrogenase gene (Fig. 7) even when the starting cDNAs were also diluted serially (data not shown). Irak2c expression is therefore regulated by LPS and may be involved in a negative feedback loop on LPS signaling.

DISCUSSION

Here, we report an unexpected complexity in TLR signaling by the identification of four naturally occurring isoforms of Irak2, which we have named Irak2a, 2b, 2c, and 2d. The diversification of Irak2 appears to occur during the processes that lead to the generation of *Irak2* mRNA. The alternative splicing of the *Irak2* gene is not the first case reported for genes encoding TLR signaling proteins. Both human IRAK1 and MyD88 have been shown previously to exist as multiple isoforms generated by alternative splicing (8, 10). The full-length Irak2a isoform is the murine orthologue of IRAK2 and is almost identical to the single Irak2 described previously (18). The observed sequence differences are most likely due to artifacts generated by the RT-PCR reactions used by these authors, and the primers employed would only amplify Irak2a and/or Irak2d rather than all four isoforms.

The four isoforms of Irak2 isolated are generated by alternative splicing and migrate at an mRNA mobility of ~3.5 kb because of the relatively similar sizes of their respective cDNAs and the level of resolution to which Northern blots can attain. We were therefore unable to distinguish the *Irak2* splice variants by Northern blotting, and the lack of availability of an antibody precluded us from analyzing endogenous Irak2 protein expression. The mRNA expression profile of *Irak2* that we generated differed from the reported human *IRAK2* expression profile (4). *Irak2* mRNA, compared with human *IRAK2* mRNA, was less abundant in lung, skeletal muscle, and spleen.

Functional analysis of the Irak2 isoforms using an LPS-responsive NF-κB reporter demonstrated that the full-length Irak2a was able to positively regulate LPS responses. This activity appeared to be mediated primarily by the death domain, because the natural truncation mutants of Irak2 that lack this domain (Irak2c and Irak2d) acted as inhibitors of LPS-induced NF-κB activity. These data suggest that Irak2c and 2d are endogenous inhibitors of LPS signaling and, if induced during signaling, would act in a negative feedback manner. This was further suggested when we examined the regulatory regions of the Irak2 variants and, as a consequence, the regulation of expression of Irak2a and Irak2c. Two *Irak2* 5′-UTRs are present; one is utilized by *Irak2a, 2b*, and *2d*, and the other, ~30 kb 3′ of this, is utilized solely by *Irak2c*. This finding strongly suggested that separate promoters, perhaps in response to entirely different stimuli, regulate these isoforms. This was reflected by the putative transcription factor binding sites identified in each 5′-flanking region. The putative *Irak2c* promoter, unlike the putative promoter for the other Irak2 isoforms, is predicted to contain binding sites for transcription factors implicated in innate immune responses such as NF-κB, signal transducers and activators of transcription 1, interferon regulatory factor 7, and an interferon-stimulated response element. We therefore explored whether LPS might induce *Irak2c*, rather than *Irak2a* mRNA and found that was indeed the case, suggesting differential regulation of Irak2 isoforms.

It is therefore likely that Irak2a and Irak2b mediate signaling by TLRs, with the induction of Irak2c occurring rapidly during signaling and having a modulatory role on the TLR pathway. This is somewhat similar to the case of $MyD88_S$, which is generated during signaling and has a negative effect on NF-κB activation (8–9). Alternative splicing of IRAK2 does not occur in humans. The question therefore arises as to why mice require this additional level of control. Other differences have been found in the TLR system between humans and mice. Two examples are TLR11, a pattern recognition receptor for uropathogenic bacteria that was found to be non-functional in humans (26), and TLR8, which is non-functional in mice (27). All of these differences probably arose during the evolution of the innate defense systems of each species in response to selective pressure applied by different pathogens. Caution should therefore be applied when extrapolating data from mice to humans in the TLR system. It may be possible, however, to devise strategies to limit human IRAK2 by using the complexity of murine Irak2 as a lead. Future interspecies comparisons will provide insights into the regulation and evolution of the TLR system in mammals.

REFERENCES

1. Dunne, A., and O'Neill, L. (2003) *Science's STKE* http://stke. sciencemag. org/cgi/content/full/sigtrans;2003/171/re3
2. O'Neill, L., Fitzgerald, K., and Bowie, A. (2003) *Trends Immunol.* **24,** 286–290
3. Cao, Z., Henzel, W. J., and Gao, X. (1996) *Science* **271,** 1128–1131
4. Muzio, M., Ni, J., Feng, P., and Dixit, V. M. (1997) *Science* **278,** 1612–1615
5. Wesche, H., Gao, X., Li, X., Kirschning, C. J., Stark, G. R., and Cao Z. (1999) *J. Biol. Chem.* **274,** 19403–19410
6. Li, S., Strelow, A., Fontana, E. J., and Wesche, H. (2002) *Proc. Natl. Acad. Sci. U. S. A.* **99,** 5567–5572
7. Li, X., Commane, M., Burns, C., Vithalani, K., Cao, Z., and Stark, G. R. (1999) *Mol. Cell. Biol.* **19,** 4643–4652
8. Janssens, S., Burns, K., Tschopp, J., and Beyaert, R. (2002) *Curr. Biol.* **12,** 467–471
9. Janssens, S., Burns, K., Vercammen, E., Tschopp, J., and Beya (2003) *FEBS Lett.* **548,** 103–107
10. Jensen, L. E., and Whitehead, A. S. (2001) *J. Biol. Chem.* **276,** 29037–29044
11. Heinemeyer, T., Wingender, E., Reuter, I., Hermjakob, H., Kel, A., Kel., O., Ignatieva, E., Ananko, E., Podkolodnaya, O., Kolpakov, F. A., Podkolodny, N. L., and Kolchanov, N. A (1998) *Nucleic Acids Res.* **26,** 362–367
12. Quandt, K., Frech, K., Karas, H., Wingender, E., and Werner, T. (1995) *Nucleic Acids Res.* **23,** 4878–4884
13. Bray, N., Dubchak, I., and Pachter, L. (2003) *Genome Res.* **13,** 97
14. Dubchak, I., Brudno, M., Loots, G. G., Pachter, L., Mayor, C., Rubin, E. M., and Frazer, K. A. (2000) *Genome Res.* **10,** 1304–1306
15. Mayor, C., Brudno, M., Schwartz, J. R., Poliakov, A., Rubin, E. M., Frazer K. A., Pachter, L. S., and Dubchak, I. (2000) *Bioinformatics* **16,** 1046–1047
16. Sigrist, C. J., Cerutti, L., Hulo, N., Gattiker, A., Falquet, L., Pagni, M., Bairoch, A., and Bucher, P. (2002) *Brief. Bioinformatics* **3,** 265–274

17. Hardy, M. P., Hertzog, P. J., and Owczarek, C. M. (2002) *Biochem. J.* **365,** 355–367
18. Rosati, O., and Martin, M. U. (2002) *Biochem. Biophys. Res. Commun.* **297,** 52–58
19. Shapiro, M., and Senapathy, P. (1987) *Nucleic Acids Res.* **15,** 7155–7174
20. Loots, G., Locksley, R., Blankespoor, C., Wang, Z., Miller, W., Rubin, E., and Frazer, K. (2000) *Science* **288,** 136–140
21. Kunsch, C., Ruben, S., and Rosen, C. (1992) *Mol. Cell. Biol.* **12,** 4412–4421
22. Grilli, M., Chiu, J., and Lenardo, M. (1993) *Int. Rev. Cytol.* **143,** 1–62
23. Horvath, C., Wen, Z., and Darnell, J., Jr. (1995) *Genes Dev.* **9,** 984–994
24. Lin, R., Genin, P., Mamane, Y., and Hiscott, J. (2000) *Mol. Cell. Biol.* **20,** 6342–6353
25. Levy, D. E., Kessler, D. S., Pine, R., Reich, N., and Darnell, J. E., Jr. (1988) *Genes Dev.* **2,** 383–393
26. Zhang, D., Zhang, G., Hayden, M. S., Greenblatt, M. B., Bussey, C., Flavell, R. A., and Ghosh, S. (2004) *Science* **303,** 1522–1526
27. Heil, F., Hemmi, H., Hochrein, H., Ampenberger, F., Kirschning, C., Akira, S., Lipford, G., Wagner, H., and Bauer, S. (2004) *Science* **303,** 1526–1529